

Molecular orientation of CN adsorbed on Pd(110)

F. Bondino, E. Vesselli, A. Baraldi, G. Comelli, A. Verdini, A. Cossaro, L. Floreano, and A. Morgante

Citation: *The Journal of Chemical Physics* **118**, 10735 (2003); doi: 10.1063/1.1574794

View online: <http://dx.doi.org/10.1063/1.1574794>

View Table of Contents: <http://scitation.aip.org/content/aip/journal/jcp/118/23?ver=pdfcov>

Published by the [AIP Publishing](#)

Articles you may be interested in

[Synthesis and characterization of oriented graphitelike B–C–N hybrid](#)

J. Appl. Phys. **99**, 084902 (2006); 10.1063/1.2189008

[C 70 adsorbed on Cu\(111\): Metallic character and molecular orientation](#)

J. Chem. Phys. **116**, 7685 (2002); 10.1063/1.1467346

[Functionalization of silicon step arrays II: Molecular orientation of alkanes and DNA](#)

J. Appl. Phys. **90**, 3291 (2001); 10.1063/1.1397297

[Scanning tunneling microscopy study of the molecular arrangement of meta- and para-xylene on Pd\(111\)](#)

J. Vac. Sci. Technol. A **19**, 1993 (2001); 10.1116/1.1366698

[Orientation and symmetry of ethylene on Pd\(110\): A combined HREELS and NEXAFS study](#)

J. Chem. Phys. **112**, 5948 (2000); 10.1063/1.481168



Molecular orientation of CN adsorbed on Pd(110)

F. Bondino,^{a)} E. Vesselli,^{b)} A. Baraldi,^{b)} G. Comelli,^{b)} A. Verdini, A. Cossaro,^{b)} L. Floreano, and A. Morgante^{b)}

Laboratorio TASC-INFN, s.s. 14 Km 163.5 in Area Science Park, 34012 Trieste, Italy

(Received 2 December 2002; accepted 25 March 2003)

The bonding geometry of the C–N molecule in the saturated $c(2 \times 2)$ layer on the Pd(110) surface has been determined by combining polarization-dependent near edge x-ray absorption fine structure and full-solid-angle x-ray photoelectron diffraction (PED). The N K -edge spectra display a strong dependence on the polar and azimuthal orientation of the light polarization with respect to the sample surface. A strong forward scattering peak along the [001] direction is present in the full-solid-angle photoelectron diffraction data of the C1s core level. Both the position of the C1s PED forward scattering peak and the angular dependence of the N K -shell absorption spectra provide direct evidence that the CN molecules is oriented with the molecular axis along the [001] surface direction, at variance with earlier conclusions based on angle-resolved valence level photoemission data. The forward scattering peak in the C1s PED data further indicates that the N atoms lie above the C atoms, with the C–N molecular axis tilted by $25^\circ \pm 4^\circ$ with respect to the surface plane. The close analogy of this geometry with the results of previous structure determinations of CN adsorbed on Ni and Rh (110) surfaces is discussed. © 2003 American Institute of Physics. [DOI: 10.1063/1.1574794]

I. INTRODUCTION

CN is an interesting molecule having a model character for the surface interactions of organic and polymeric nitriles, where the CN functional groups provide important centers for surface attachment.¹

Moreover, the formation of cyanide intermediates has been detected in the catalytic reduction of NO by C₂H₄,² in the reaction between NO and carbon,³ in the reaction of CO with coadsorbed nitrogen⁴ or NO, both on supported catalysts⁵ and single crystals.⁶ The formation of these cyanide intermediates is an unwanted reaction step in the removal of NO by the three-way catalyst, mostly composed of supported transition metal particles such as Pt, Pd, and Rh on Al₂O₃ or SiO₂, since part of the adsorbed CN hydrogenates and desorbs as poisonous HCN, while the remainder decomposes, shifting the desorption of N₂ to higher temperatures.

On metal surfaces in ultra-high vacuum environment the CN bonding geometry is rather peculiar. Unlike most adsorbed diatomic molecules (i.e., CO, NO, N₂, etc.)⁷ and contrary to expectations drawn from coordination chemistry,⁸ on most metal-vacuum interfaces CN does not bind in the typical end-on geometry, but with the molecular axis essentially parallel to the surface.^{9–18}

Full quantitative structural determinations of the CN adsorption geometry are limited to two studies, on Ni(110) using near edge x-ray absorption fine structure (NEXAFS) and photoelectron diffraction (PED)⁹ and on Rh(110) using dynamical low energy electron diffraction (LEED).¹⁸ In both cases the C–N molecular axis was found to be aligned along

the surface [001] direction, tilted by approximately 20° from the surface plane. On Pd(110), CN species, originated by complete dissociation of C₂N₂ at room temperature, form an ordered $c(2 \times 2)$ layer at saturation. In this case, indirect information on the CN adsorption geometry was previously derived from ARUPS data.¹¹ The lift of the π orbital degeneracy in ARUPS data¹¹ indicated that CN is bonded either parallel to the surface or with a significant tilt from the surface normal. Previously, ARUPS was also used to determine the orientation of CN species on Ni(110).¹² The ARUPS data of CN on Pd(110) and on Ni(110) show almost identical angular dependence of the photoemission features. In both cases, ARUPS data were interpreted in terms of CN axis aligned along the $[1\bar{1}0]$ direction. However, this conclusion was questioned by a recent NEXAFS and PED measurements of $c(2 \times 2)$ -CN on Ni(110), which indicated a CN axis oriented along the surface [001] direction.¹³

Here we report on the measurement of the angular dependence of NEXAFS N K -edge resonance intensities and the angular dependent distribution of the photoelectron intensity of $c(2 \times 2)$ -CN on Pd(110). The conclusions derived both from PED and NEXAFS data are consistent and provide the azimuthal orientation and the tilt angle of the CN molecules relative to the Pd(110) substrate. The results of the present work confirm the nearly parallel bonding configuration of CN species on Pd(110) deduced from ARUPS data, but indicate a [001] azimuthal orientation of the C–N molecular axis, at variance with ARUPS results.

II. EXPERIMENT

The experiments were performed at the ALOISA beam-line^{19–21} of ELETTRA, the Trieste synchrotron facility.

^{a)}Author to whom correspondence should be addressed. Electronic mail: bondino@tasc.infn.it

^{b)}Also at: Dipartimento di Fisica, Università di Trieste, Via Valerio 2, 34127 Trieste, Italy.

Sample position was set automatically using a modified VG-CTPO motorized manipulator with six degrees of freedom, which allows to freely select, with 0.01° accuracy, the orientation of both the photon beam grazing angle (0° – 10°) and of the sample surface with respect to the radiation polarization vector.

At the same time, the emission direction can be chosen with high flexibility, since a wide portion of the full-solid angle above the sample can be probed for any surface orientation, thanks to the combined rotation of the frame hosting the analyzer and of the whole experimental chamber. The photon beam is linearly polarized with the electric field vector in the horizontal plane.

Scanned-angle PED patterns were obtained by measuring $C1s$, $N1s$, and $Pd3d_{5/2}$ signal at the peak energy maximum and at an additional higher kinetic energy value aside the peak to obtain reference data for linear background subtraction. The photon-beam grazing angle was set to 4° with the electric field vector parallel to the surface plane, i.e., in transverse electric (TE) polarization. Automatic angular scans were performed by computer-controlled stepping motors rotating the detector in a plane perpendicular to the scattering one by varying the emission angle θ from the surface normal ($\theta=0^\circ$) to the grazing emission ($\theta=84^\circ$) with 1° constant θ steps and rotating the sample around the surface normal by varying the azimuthal angle ϕ with 2° constant ϕ steps from -10° to 100° with respect to the Pd surface $[001]$ direction [Fig. 1(a)]. The azimuthal angle ϕ was scanned over a range of 110° , which includes all the features of the full-solid-angle pattern, due to the $\pi/2$ symmetry of the surface. The full-solid-angle PED pattern was obtained by a symmetric extension of the measured $\pi/2$ portion.

During the PED scans the precession of the surface normal due to some residual misalignment of the crystal on the sample holder was automatically corrected. The required corrections were preliminarily determined by measuring the beam specular reflectivity from the sample surface using a diode detector.

The PED plot presented in the following shows the intensity in a linear gray scale of $C1s$ core level. Each point in the displayed patterns shows the intensity measured at a specific (θ, ϕ) angular position, in a polar coordinate system, where θ is the radial distance from the center of the plot. The center of the plot corresponds to normal emission and the circumference to grazing emission. For each polar angle, the PED data have been normalized to the average intensity calculated over the azimuthal scan.

The absorption at the nitrogen K -edge was measured by recording the intensity of the nitrogen KVV Auger electron transition as a function of the photon energy. Auger and photoemitted electrons were collected with a 35 mm mean radius hemispherical analyzer with $\sim 1^\circ$ acceptance angle.²² All NEXAFS spectra were normalized to the photon flux, scaled to the same intensity before the absorption and finally background subtracted by fitting the data in the pre-edge region. Polarization-dependent NEXAFS experiments were performed by rotating either the sample and the whole chamber together around the beam axis or the sample around the sur-

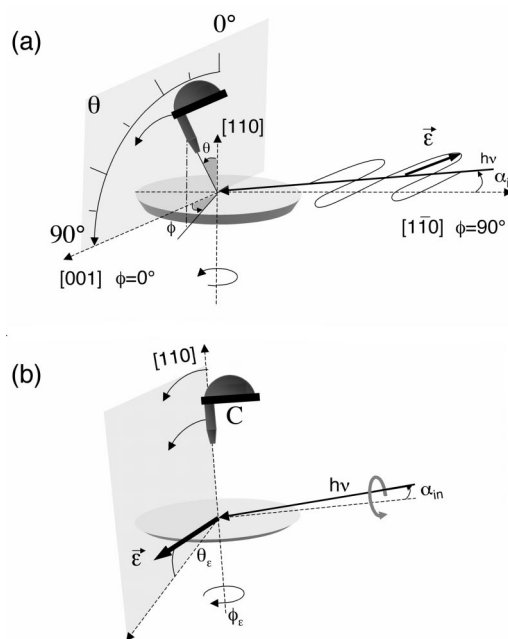


FIG. 1. (a) Experimental set up for full-solid-angle PED data acquisition at the ALOISA end-station. The azimuthal angle ϕ of the analyzer was varied by rotating the sample around its normal. The polar angle θ of the analyzer was varied by rotating the chamber hosting the analyzer around the beam axis in the plane highlighted in the figure. The grazing incidence angle (α) was fixed and the polarization vector was parallel to the surface plane. (b) Sketch of the experimental geometry used for the acquisition of the Auger Yield NEXAFS spectra. θ_ϵ is the angle of the polarization from the surface plane. ϕ_ϵ is the azimuthal angle of the polarization with respect to the Pd surface $[001]$ direction. At fixed $\phi_\epsilon=0$, the angle θ_ϵ was varied by rotating the sample by $\Delta\theta_\epsilon$ around the beam axis. At the same time the chamber hosting the analyzer (C) was rotated by the same amount ($\Delta\theta_\epsilon$) around the beam axis, in order to have a constant emission angle for all the spectra with different θ_ϵ . At fixed θ_ϵ , ϕ_ϵ was changed by rotating the sample around the surface normal, while keeping the polarization $\vec{\epsilon}$ vector parallel to the surface ($\theta_\epsilon=0$, TE polarization). In both cases, the grazing incidence angle (α_{in}) was fixed.

face normal, keeping the sample in TE polarization [Fig. 1(b)].

The cleaning procedure of the Pd(110) surface involved repeated cycles of Ar ion bombardment at room temperature and annealing to 1050 K, followed by oxygen treatment at 625 K and reduction in hydrogen, until the surface exhibited a sharp 1×1 reflection high energy electron diffraction (RHEED) pattern and no traces of contaminants were detected by photoemission. The azimuthal orientation of the surface was evaluated using RHEED.

Cyanogen (C_2N_2) was produced by thermal decomposition of AgCN in a tube attached to the gas line; the gas was dosed by background exposure via a leak valve.

The saturation $c(2 \times 2)$ -CN/Pd(110) adlayer was produced by dosing 10 L of C_2N_2 at 325 K sample temperature. At this temperature C_2N_2 adsorbs dissociatively as a single CN species.²³ In agreement with previous LEED investigations of the saturated CN layer,¹¹ we observed by RHEED an ordered $c(2 \times 2)$ periodicity.

Background pressure in the UHV chamber, during the measurements, was always in the low 10^{-10} mbar range. All measurements were collected at room temperature.

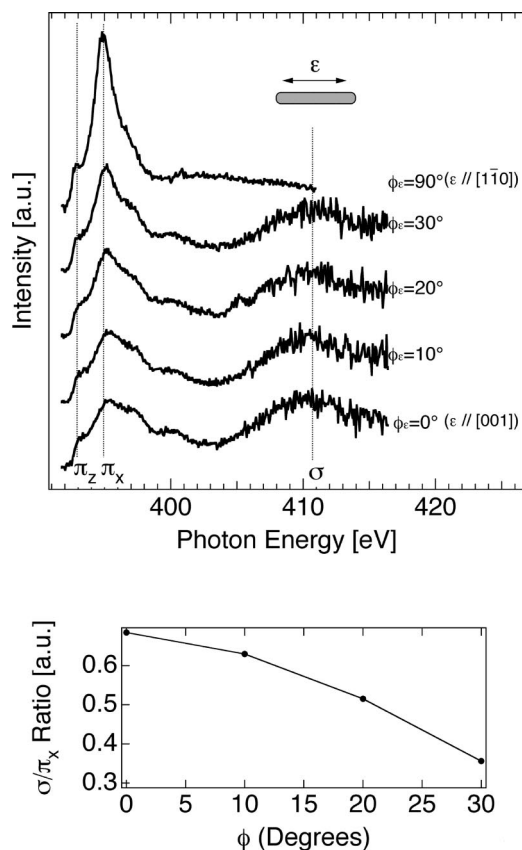


FIG. 2. Top: set of Auger yield N *K*-shell NEXAFS spectra recorded as a function of the light-polarization azimuthal angle (ϕ_e), with the electric field in the surface plane (TE polarization).

III. RESULTS AND DISCUSSION

A. NEXAFS

Figure 2 displays a set of N *K*-shell NEXAFS spectra, measured with the electric field ϵ in the surface plane ($\theta_e = 0^\circ$, TE polarization) at different azimuthal angles ϕ_e , where ϕ_e is the angle between ϵ and the [001] direction [Fig. 1(b)]. The NEXAFS spectra were measured by recording the Auger KVV intensity with the electron analyzer aligned along the surface normal. The main peaks in the spectra are very similar to the features present in the corresponding N *K*-edge NEXAFS spectra of CN on Ni(110)⁹ and CN on Pd(111).¹⁴ A single sharp peak close to 395 eV with a small shoulder at 393 eV is observed when the electric vector is oriented along the [1 $\bar{1}$ 0] direction of the surface plane. In accordance with previous studies, the sharp peak close to 395 eV is assigned to a $1s \rightarrow \pi^*$ transition.

By changing the azimuthal orientation of the electric field vector from the [1 $\bar{1}$ 0] to the [001] direction, the intensity of the π^* resonance decreases and a broad feature grows up at 15 eV higher photon energy. The energy position of the broad feature is consistent with the location of the σ^* shape resonance observed in gas-phase NEXAFS spectra of molecules containing the CN group²⁴ and with the feature observed in the NEXAFS spectra of CN on Ni(110) and Pd(111).^{9,14} Although the assignment of the features above the photoionization threshold should be approached with

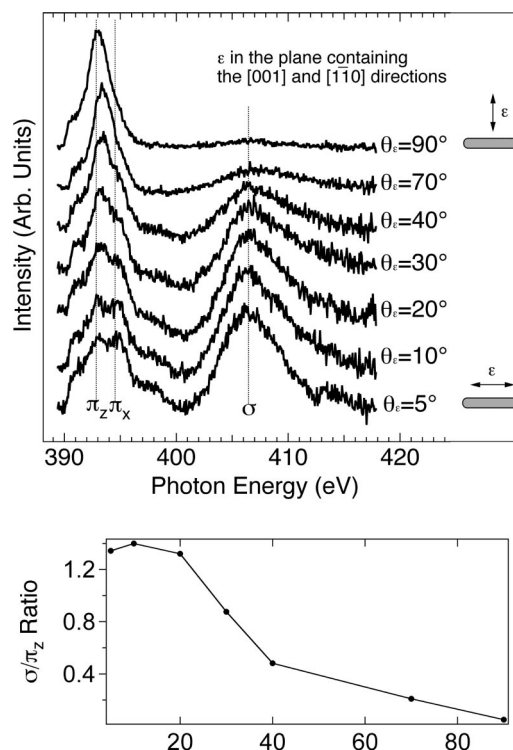


FIG. 3. Top: set of Auger yield N *K*-shell NEXAFS spectra recorded as a function of the light-polarization polar angle (θ_e), at fixed surface azimuthal orientation (ϵ along the [001] direction), fixed photon incidence (4°) and with the analyzer kept nearly normal to sample surface. Bottom: plot of the σ^*/π_z^* intensity ratio as a function of the light-polarization polar angle.

care and should be verified by single hole cross-section measurements,²⁵ in agreement with previous studies, we assign the broad feature at 410 eV to the transition to a σ^* shape resonance. Notice that, in the spectrum measured with the electric field along the [1 $\bar{1}$ 0] direction, the 410 eV broad peak is not present. The plot of the σ^*/π_z^* intensity ratio as a function of the azimuthal angle of the polarization is displayed in the bottom panel of Fig. 2. The azimuthal dependence of the NEXAFS spectra and, in particular, the inequivalence of the [001] and [1 $\bar{1}$ 0] directions, clearly indicate that the C–N molecular axis is not perpendicular to the surface.

Further evidence of this conclusion is derived from the series of Auger yield N *K*-edge spectra measured as a function of the beam-polarization polar angle, at fixed surface azimuthal orientation (ϵ along the [001] direction), fixed photon incidence (4°) and with the analyzer near to the sample normal (Fig. 3).

The orientation of the linear light polarization was changed from perpendicular to [$\theta_e = 90^\circ$, i.e., transverse magnetic (TM) polarization] polar nearly parallel to the surface plane ($\theta_e = 5^\circ$, \sim TE polarization) by simultaneously rotating the sample and the chamber around the beam axis while keeping the incidence photon beam angle and the emission direction fixed with respect to the sample surface [see Fig. 1(b)].

The spectra display a strong angular dependence. At $\theta_e = 90^\circ$ only the π^* resonance at 393 eV is present. By changing the polar orientation of the electric field vector from 90°

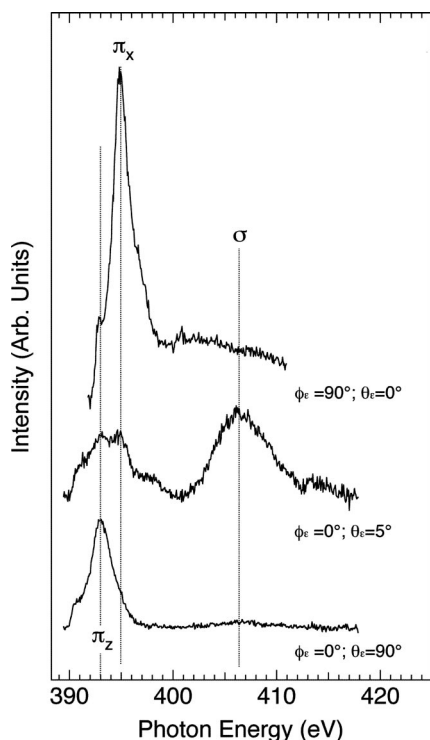


FIG. 4. Comparison of the NEXAFS spectra measured for ε along the (a) $[1\bar{1}0]$, (b) $[001]$, (c) $[110]$ directions of the sample.

to 5° the π^* component intensity decreases and the σ^* shape resonance grows up.

According to the dipole selection rules governing the K -shell NEXAFS resonances,²⁶ the intensity associated with a specific molecular orbital is largest if the electric vector of the light points in the direction of that molecular orbital and it vanishes when the electric vector is perpendicular to that orbital. In our case the π^* states can only be excited when the electric vector is perpendicular to the C–N molecular axis, proving therefore that the molecular orientation is highly tilted ($\approx 70^\circ$ – 80°) from the surface normal. Furthermore, from the azimuthal-dependent NEXAFS spectra shown in Fig. 2, it can be concluded that the CN species are azimuthally aligned along the $[001]$ direction.

In Fig. 4 the NEXAFS spectra measured for ε along the sample normal and for ε along the sample $[1\bar{1}0]$, $[001]$ directions are compared.

By labeling the $[1\bar{1}0]$, $[001]$ and surface normal directions as x , y , and z , respectively, the single sharp resonant peak observed for ε perpendicular to the surface is assigned to the $1s \rightarrow \pi_z^*$ excitation, while the sharp resonance appearing in the spectrum recorded with ε along the $[1\bar{1}0]$ direction in the surface plane is assigned to a $1s \rightarrow \pi_x^*$ excitation.

The energy position of the π_x^* resonance (observed at $\theta_\varepsilon = 0^\circ$, $\phi_\varepsilon = 90^\circ$) and the π_z^* excitation (visible at $\theta_\varepsilon = 90^\circ$) differs by ~ 2 eV. The lifting of the degeneracy of the two π^* orbitals is consistent with a configuration where the C–N molecular bond is lying in a plane parallel or nearly parallel to the surface because the π_z^* molecular orbitals interact directly with the substrate. We further observe that in the spectrum at $\theta_\varepsilon = 5^\circ$, $\phi_\varepsilon = 0^\circ$, the intensity of π_z^* is much

reduced and the π^* resonance is clearly splitted in two components. The component located at 2 eV higher photon energy can be assigned to residual π_x^* intensity. Correspondingly, the component at 2 eV lower energy with respect to the main peak in the spectrum measured at $\theta_\varepsilon = 0^\circ$, $\phi_\varepsilon = 90^\circ$ is associated with residual π_z^* intensity. Thus, it is clear that the C–N molecular bond lies in a plane parallel or nearly parallel to the surface approximately oriented along the $[001]$ direction, even if residual π_x and π_z intensities are present for geometries where they should be absent according the selection rules for NEXAFS resonances. In particular, the presence of the feature assigned to π_x for ε oriented along y , i.e., the $[001]$ direction, could be due to a vibrational motion of the nitrogen atom or to a twist of the CN bond from the $[001]$ direction. The presence of the π_z for ε parallel to surface could be either due to a static tilt of the CN bond from sample plane or to the residual unpolarized light or to vibrational motions of the nitrogen atom or a combination of these factors.²⁷

From a simple visual inspection of the NEXAFS spectra, the orientation of the CN molecular axis has been qualitatively determined. A quantitative analysis of the NEXAFS data must be approached with care for the difficulty implied in handling the normalization, background corrections and deconvolution of the different effects (imperfect light polarization, vibrations). A rough estimate of the orientation of C–N bond axis has been derived from the evaluation of the σ^*/π^* intensity ratio with the electric vector orientation in the angle-dependent near-edge spectra, by fitting the π^* peaks with Gaussian functions and the σ^* resonance with Gaussian functions having a width linearly dependent on the photon energy, as proposed by Outka and Stöhr.²⁸ Neglecting the degree of linear polarization, the σ^*/π^* intensity ratio indicates that the C–N bond lies along the $[001]$ direction, tilted by approximately $15^\circ \pm 10^\circ$ from the surface plane.

Another set of N K -edge data was collected using total electron yield (TEY) detection mode. Except for the TEY mode giving a much smaller signal to background ratio, the same behavior of the π^* and σ^* resonances as a function of the electric field orientation with respect to the surface normal was found.

B. Full-solid-angle PED

The experimental full-solid-angle PED pattern, measured for $C1s$ with photon energy of 947 eV in TE polarization, i.e., with the photon polarization vector parallel to the surface plane, is reported in Fig. 5.

The most prominent feature appearing in the experimental PED pattern is a strong peak along the surface $[001]$ direction, at approximately 25° from the sample plane. Because of the high kinetic energy of the photoelectrons, this peak can be safely attributed to forward scattering of $C1s$ electrons due to other atoms located at a higher vertical position.

The possibility that the scatterer atom is a first layer Pd atom can be excluded with the following considerations. A forward scattering peak due to scattering between C and Pd atoms would be present in the same azimuthal position if the

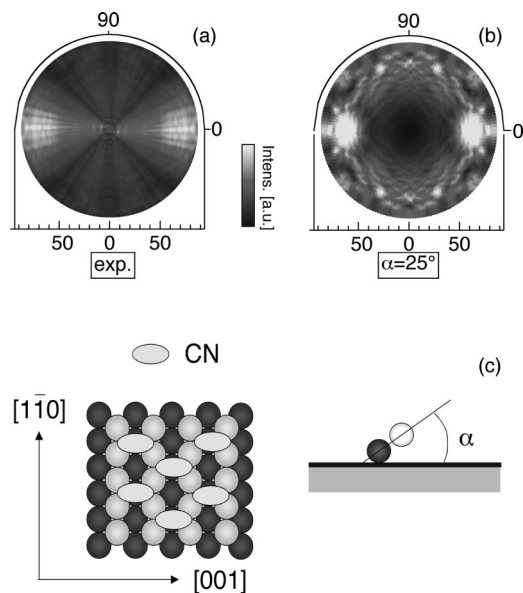


FIG. 5. Full-solid-angle $C1s$ PED pattern measured at 947 eV photon energy (a) with the PED simulation obtained for a C–N tilt angle of 25° from the surface plane (b). Each point in the displayed patterns shows the normalized intensity in a linear gray scale of the $C1s$ core level measured at a specific (θ, ϕ) angular position, in a polar coordinate system, where θ is the radial distance $[1\bar{1}0]$ directions, respectively. (c) Schematic representation of the CN adsorption geometry as derived from PED and NEXAFS measurements.

C atoms were located at bridge sites on the second Pd layer, below the first Pd atomic layer. However, considering a rough estimation based on the covalent radii of C and Pd (refraction effects can be neglected at these energies), the polar position of this peak would be at much grazing emission ($\sim 0^\circ$ – 5° from the sample plane) than that observed ($\sim 25^\circ$). Therefore, the scatterer atom responsible for the forward scattering enhancement is likely to be the nitrogen atom bonded to the emitting carbon. This implies that the C–N bond is oriented along the surface $[001]$ direction, with the C–N axis inclined from the surface plane and that the C atoms are closer to the surface than the N atoms.

An analogous $N1s$ full-solid-angle PED pattern collected using photon energy of 810 eV in TE polarization did not show the presence of any forward scattering features, but it appeared uniform over all the measured region. The lack of forward scattering features further strengthens the conclusion derived from $C1s$ PED data, that the N atoms lie above the emitting C atoms.

The azimuthal position of the peak with respect to the substrate directions is determined accurately by recording simultaneously the $C1s$ and $Pd3d_{5/2}$ signal during PED data acquisition.

To derive quantitatively the C–N bond orientation, single scattering calculations have been performed using the MSCD code²⁹ at several tilt angles (α) of the C–N bond oriented along the $[001]$ direction. The simulations take into account the symmetry of the outgoing wave, refraction at the surface potential step, inelastic effects and isotropic vibrations of the atoms. The existence of two equally populated CN domains has been considered both in the PED calcula-

tions and in the symmetric mapping of the $\pi/2$ angular portion of experimental data. The best agreement between experimental and theoretical data, in particular concerning the forward scattering peak position, was found for $\alpha = 25^\circ \pm 4^\circ$. The corresponding calculated PED pattern is reported in Fig. 5(b).

Since the measurements were collected at room temperature, we point out that anisotropic vibrations of the scatterer, e.g., a hindered translation of CN along the $[001]$ direction and possible differences in the vibrational amplitudes in the $[001]$, $[1\bar{1}0]$, and $[110]$ directions, which have not been accounted in our analysis, could affect the value of the tilt of the CN molecular axis derived from PED and NEXAFS data with the assumption of static molecules.

This determination of the C–N molecular bond orientation indicates that CN on Pd(110) follows the general adsorption behavior of CN species, preferentially bonded with C–N axis nearly parallel to the surface in metal-vacuum interfaces. In particular, the intramolecular orientation of CN on Pd(110) is consistent with that of CN on Ni(110) determined by photoelectron diffraction⁹ and CN on Rh(110) determined by LEED-*IV*.¹⁸ In both cases the molecule was found to be located within the (110) grooves, on top of a second layer substrate atom, oriented along the $[001]$ direction, with the nitrogen atom bridging two first layer metal atoms and the carbon atom bound to both the first and second layer metal atoms. Thus, CN adsorbed molecules display a general preference towards an alignment along the $[001]$ direction on all the investigated (110) transition metal surfaces.

The CN lying-down configuration has been tentatively attributed to strong electrostatic and polarization contributions as CN^- binds to metal surfaces.³⁰ The adsorption configuration found on Pd(110), Ni(110), and Rh(110) is consistent with a threefold coordination and a combined π and σ bonding. This preferential adsorption geometry could be used as a starting point for the calculation of the electronic properties of the adsorbed CN species to provide a better physical and chemical insight into the intriguing nature of CN bond with metal surfaces, whose understanding is still poor.

IV. CONCLUSIONS

Information on azimuthal molecular orientation as well as on the tilt of the C–N molecular axis on the Pd(110) surface has been derived by combining angle-dependent NEXAFS and full-solid-angle PED measurements.

NEXAFS data and PED yield independent and consistent conclusions, indicating a nearly parallel CN adsorption on Pd(110), with preferential azimuthal orientation of the C–N molecular axis along the $[001]$ direction. Furthermore, the presence of a 25° tilt of the C–N axis from the surface plane is found with the C atoms closer to the surface than N ones. While the near-parallel bonding geometry of CN found by previous ARUPS data¹¹ is confirmed, the azimuthal orientation of the bond axis contradicts the conclusions based on the interpretation of photoemission data.

ACKNOWLEDGMENTS

This work was supported by the Italian INFN, by MURST under the program "COFIN01" and by Sincrotrone Trieste S.C.p.A. We gratefully acknowledge R. Gotter for technical assistance.

- ¹F.P. Netzer and M.G. Ramsey, *Crit. Rev. Solid State Mater. Sci.* **17**, 397 (1992).
- ²R.M. van Hardeveld, A.J.G.W. Schmidt, R.A. van Santen, and J.W. Niemantsverdriet, *J. Vac. Sci. Technol. A* **15**, 1642 (1997).
- ³L.A. DeLouise and N. Winograd, *Surf. Sci.* **154**, 79 (1985).
- ⁴P. Jakob, *Chem. Phys. Lett.* **263**, 607 (1996).
- ⁵D.R. Mullins, L. Kundakovic, and S.H. Overbury, *J. Catal.* **195**, 169 (2000).
- ⁶J.H. Miners, A.M. Bradshaw, and P. Gardner, *Phys. Chem. Chem. Phys.* **1**, 4909 (1999).
- ⁷H. Over, *Prog. Surf. Sci.* **58**, 249 (1998).
- ⁸A.G. Sharpe, *The Chemistry of Cyano Complexes of Transition Metals* (Academic, New York, 1976).
- ⁹N.A. Booth, R. Davis, D.P. Woodruff *et al.*, *Surf. Sci.* **416**, 448 (1998).
- ¹⁰M.E. Kordesch, W. Stenzel, and H. Conrad, *Surf. Sci.* **186**, 601 (1987).
- ¹¹M.G. Ramsey, G. Rosina, F.P. Netzer, H.B. Saalfeld, and D.R. Lloyd, *Surf. Sci.* **218**, 317 (1989).
- ¹²M.G. Ramsey, D. Steinmüller, F.P. Netzer, S. Köstlmeier, J. Lauber, and N. Rösh, *Surf. Sci.* **309**, 82 (1994).
- ¹³K. Besenthal, G. Chiarello, M.E. Kordesch, and H. Conrad, *Surf. Sci.* **178**, 667 (1986).
- ¹⁴J. Somers, M.E. Kordesch, Th. Lindner, H. Conrad, and A.M. Bradshaw, *Surf. Sci.* **188**, L693 (1987).
- ¹⁵M.E. Kordesch, Th. Lindner, J. Somers, W. Stenzel, H. Conrad, A.M. Bradshaw, and G.P. Williams, *Spectrochim. Acta, Part A* **43**, 1561 (1987).
- ¹⁶M.E. Kordesch, W. Stenzel, H. Conrad, and M. Weaver, *J. Am. Chem. Soc.* **109**, 1878 (1987).
- ¹⁷M.E. Kordesch, W. Feng, W. Stenzel, M. Weaver, and H. Conrad, *J. Electron Spectrosc. Relat. Phenom.* **44**, 149 (1987).
- ¹⁸F. Bondino, A. Baraldi, H. Over, G. Comelli, S. Lizzit, G. Paolucci, and R. Rosei, *Phys. Rev. B* **64**, 085422 (2001).
- ¹⁹L. Floreano, G. Naletto, D. Cvetko *et al.*, *Rev. Sci. Instrum.* **70**, 3855 (1999).
- ²⁰F. Bruno, L. Floreano, A. Verdini, D. Cvetko, R. Gotter, A. Morgante, M. Canepa, and S. Terreni, *J. Electron Spectrosc. Relat. Phenom.* **127**, 85 (2002).
- ²¹Details about the experimental chamber can be found at <http://www.tasc.infn.it/tasc/lds/aloisa/aloisa.html>
- ²²R. Gotter, A. Ruocco, A. Morgante, D. Cvetko, L. Floreano, F. Tommasini, and G. Stefani, *Nucl. Instrum. Methods Phys. Res. A* **467**, 1468 (2001).
- ²³A. Baraldi, S. Lizzit, M.G. Ramsey, and F.P. Netzer, *Surf. Sci.* **416**, 214 (1998).
- ²⁴P. Hitchcock, M. Tronc, and A. Modelli, *J. Phys. Chem.* **93**, 3068 (1989).
- ²⁵B. Kempgens, H.M. Köppe, A. Kivimaki, M. Neeb, K. Maier, U. Hergen-hahn, and A.M. Bradshaw, *Phys. Rev. Lett.* **79**, 35 (1997).
- ²⁶J. Stöhr, *NEXAFS Spectroscopy* (Springer-Verlag, Berlin, 1992).
- ²⁷M. Pérez Jigato, W.K. Walter, and D.A. King, *Surf. Sci.* **301**, 273 (1994).
- ²⁸D.A. Outka and J. Stöhr, *J. Chem. Phys.* **88**, 3539 (1988).
- ²⁹MSCD code, Y. Chen and M.A. Van Hove (private communication), <http://electron.lbl.gov/mscdpack/>; Y. Chen, F.J. Garcia de Abajo, A. Chassé, R.X. Ynzunza, A.P. Kaduwela, M.A. Van Hove, and C.S. Fadley, *Phys. Rev. B* **58**, 13121 (1998).
- ³⁰K. Hermann, W. Müller, and P.S. Bagus, *J. Electron Spectrosc. Relat. Phenom.* **39**, 107 (1986).